BNL-66139

CONF-990514--

Submitted to the Electrochemical Society for the Lithium Proceedings Volume of the 195th Meetings (Seattle, Washington, May 2-7, 1999)

In Situ X-ray Diffraction Studies of a New $LiMg_{0.125}Ti_{0.125}Ni_{0.75}O_2$ Cathode Material

X. Q. Yang, X. Sun, and J. McBreen
Brookhaven National Laboratory, Upton, NY 11973

Yuan Gao and M. V. Yakovleva
FMC Corporation, Princeton, NJ 08543

X. K. Xing and M. L. Daroux
Gould Electronics Inc., Eastlake, OH 44095-4001

S. Mukerjee
Department of Chemistry, Northeastern University, Boston, MA 02115-5000

ABSTRACT

A Synchrotron x-ray source was used for ***In Situ*** x-ray diffraction studies during charge on a new $LiMg_{0.125}Ti_{0.125}Ni_{0.75}O_2$ cathode material synthesized by FMC Corp. It had been demonstrated by Gao[1] that this new material has superior thermal stability than $LiNiO_2$ and $LiCo_{0.2}Ni_{0.8}O_2$ at over-charged state. In this current paper, studies on the relationship between the structural changes and thermal stability at over-charged state for these materials are presented. For the fist time, The thermal stability of these materials are related to their structural changes during charge, especially to the formation and lattice constant change of a hexagonal phase (H3). The spectral evidence support our hypothesis that the improvement of thermal stability is obtained by suppressing the formation of H3 phase and reducing the shrinkage of its lattice constant "c" when charged above 4.3 V.

INTRODUCTION

In order to expand the application of lithium-ion batteries into the wide range of consumer electronics and electric vehicles in the future, developing safer, cheaper, and better cathode materials for these batteries become more and more important. $LiMn_2O_4$ is a cheaper and safer material but suffers from its low capacity (148 mAh/g theoretical and 115 mAh/g practical). $LiCoO_2$ is the most widely used cathode material in commercial lithium battery cells. However, only less than 60% of the theoretical capacity of 275 mAh/g can be utilized. Because further removal of lithium not only degrade the cycleablity but also causes decomposition of the oxide at elevated temperatures. The oxygen released from this reaction can react with electrolyte and poses safety problems[2,3]. $LiNiO_2$ is a less expensive material than the $LiCoO_2$ with the same theoretical capacity. However it application in lithium batteries has not been realized due to the more serious safety concerns, because it exhibits a sharper exothermic reaction with electrolyte at lower temperature than $LiCoO_2$. Substituting a portion of Ni in $LiNiO_2$

with other cations has been pursued to improve its safety characteristics. Ohzuku[4] synthesized a new material $LiNi_{0.75}Al_{0.25}O_2$ which is thermally more stable than $LiNiO_2$ in the fully charged state. Recently, Gao[1] published the results of a new $LiNi_{0.75}Mg_{0.125}Ti_{0.125}O_2$ material synthesized by FMC Corp with superior thermal stability and cyclebility. However, most of these works have been done on the empirical base and no systematic studies on the relationship between the thermal stability and the structural changes of the cathode during charge have been published. Exploring this relationship is very important not only in guiding the development of new materials, but also in setting the safety standards for the commercial materials being used today. The lack of works in this field is believed to be a result of technical limitation. Using the ex situ XRD technique, Ohzuku[4,5,6] has published extensive studies on these $LiNiO_2$ based materials and pointed out that keeping the lattice constant "c" of $LiNi_{0.75}Al_{0.25}O_2$ larger than 14 Å is the main reason for its high thermal stability[4]. However, the voltage range of charging was limited below 4.8 V and the nature of ex situ technique limited the ability to monitor the detail structural changes during charge. These changes at voltage above 5 V are very important to the thermal stability of these materials. Dahn[7,8] and co-workers have published several papers on the structural changes of these layered materials during charge studied by in situ XRD. However, the charging voltage was below 4.3 V restricted by the problem of beryllium window corrosion. Amatucci, Tarascon, and Klein[9] constructed an in situ XRD cell, which allows structural investigations at voltages greater than 5 V without any beryllium window corrosion and new findings in phase transitions at voltage higher than 4.3 V were reported for $LiCoO_2$ system. However, all of these in situ XRD studies using conventional x-ray sources probe the cell in reflection geometry. Therefore, the observed structural changes are basically come from the surface of the cathode, which might be different from the bulk during charge-discharge especially when the rate is high.

Taking the advantage of strong x-ray beam from the synchrotron light source, we have constructed lithium battery cells for in situ XRD study with Mylar windows replacing the beryllium windows. Some new findings on phase transitions in $Li_{1-x}NiO_2$ system during charge have been reported using this synchrotron based in situ technique[10]. The data presented in here shows clear correlation between the structural changes during cycling and the thermal stability of the cathode materials. Results of four materials with thermal stability in the order of $LiMg_{0.125}Ti_{0.125}Ni_{0.75}O_2$, $LiCoO_2$, $LiCo_{0.2}Ni_{0.8}O_2$, $LiNiO_2$ are presented with the reason of why $LiNiO_2$ is the least thermal stable material.

EXPERIMENTAL

$LiNiO_2$ and $LiCo_{0.2}Ni_{0.8}O_2$ were purchased from FMC Corp. and $LiNi_{0.75}Mg_{0.125}Ti_{0.125}O_2$ was provided by FMC. Cathodes were prepared by slurrying the active material powder with 10% PVDF (KynarFlex 2801, Atochem), and 10% acetylene black (w/w) in a fugitive solvent, then coating the mixture onto Al foil. After vacuum drying at 100 °C for 12 hours, the electrode disks (2.8 cm^2) were punched and weighed. The cathodes were incorporated into cells with a Li foil negative electrode, a Celgard separator and a 1 M $LiPF_6$ electrolyte in a 1:1 EC:DMC solvent (LP 30 from EM Industries Inc.). Mylar windows instead of beryllium windows were used in these in situ cells. All the the

DISCLAIMER

DISCLAIMER

Portions of this document may be illegible in electronic image products. Images are produced from the best available original document.

purchased materials were used as received without any treatment. A heat treatment process at 700 °C for two hours in oxygen was used before mixing for $LiNi_{0.75}Mg_{0.125}Ti_{0.125}O_2$. *In situ* XRD spectra were collected on beam line X18A at National Synchrotron Light Source (NSLS) at Brookhaven National Laboratory operated at an energy of 10375 eV (λ=1.195 Å). The step size for 2θ scan is 0.02 degree. The experimental setup was basically the same as described in our previous paper[11] and the XRD spectra were collected in transmission mode.

RESULTS AND DISCUSSION

Although the *in situ* XRD spectra were collected in a range that covered reflections from the (003) to (113) Bragg peaks for the hexagonal structure, only parts of the spectra in (003) peak region are presented in this paper. This is because that the largest lattice constant change at over-charged state occurs in "c" axis. Figure 1 shows the first charging curve of the in situ cell using $LiNiO_2$ cathode (20.7 mg active material) when charged at a constant current (0.5 mA at C/13 rate) between 3.5 V to 5.1 V. The initial voltage jump to 4.15 V is a common phenomenon on the first charge of $LiNiO_2$ cathodes when relative high charging rate is used. After that the voltage relaxed to about 3.8 V and displayed three plateaus before rising rapidly to 5.1 V. The *in situ* XRD spectra in (003) peak region are plotted in Fig. 2. The first scan was taken before charge and the last scan was taken during the relaxing period after the cell reached 5.1 V. The numbers corresponding to XRD scans in Fig. 2 are marked on the charging curve in Fig. 1. Each scan took about 1.1 hour and the increment of x value in $Li_{1-x}NiO_2$ in the consequent scans from 2 to 13 is about 0.083. The voltage of the cell at 2θ = 16 degrees is marked on each curve. The missing data in scan at 4.21 V was due to the unavailability of the x-ray beam. The incomplete spectra were kept in the plot to give correct indication of the progression of charge states. All the in situ spectra in this paper are presented in the same way. Three hexagonal phases (H1, H2, and H3) can be identified. The complete spectra and the phase transitions from H1 to H2 and then to H3 were discussed in detail in a previous publicatio[10]. (The lattice constants obtained from least square refinements were: a=2.884 Å and c=14.216 Å for H1; a=2.822 Å and c=14.400 Å for H2; and a=2.821 Å and c=13.354 Å for H3.) The interpretation of XRD patterns used in the literature as evidence for monoclinic phase formation was reexamined and seriously questioned in that paper. In this present paper, we will focus our discussion on the phase transition form H2 to H3 and its implication on thermal stability. As pointed out by Ohzuku[3], the large change in lattice constant "c" during H2 to H3 phase transition (from 14.40 Å to 13.35 Å) is responsible for the poor thermal stability and cycleability for $LiNiO_2$ cathode.

Figure 3 shows the first charging curve of the in situ cell using $LiNi_{0.8}Co_{0.2}O_2$ cathode (20.0 mg active material) when charged at a constant current (0.5 mA at C/12 rate) between 3.3 V to 5.2 V. The initial voltage jumped to 3.80 V and then relaxed to about 3.72 V, form two plateaus at 3.75 V and 4.5 V and then rapid rise to 5.2 V. The *in situ* XRD spectra are plotted in Fig. 4 for (003) peak region and Fig. 5 for (101) to (113) region. The first scan was taken before charge with open circuit voltage of 3.27 V. The last scan was taken at open circuit voltage of 4.6 V after the cell reached 5.2 V. The numbers corresponding to XRD scans in Fig. 3 are marked on the charging curve in Fig.

3. Each scan took about 0.8 hour and the increment of x value in $Li_{1-x}Ni_{0.8}Co_{0.2}O_2$ in the consequent scans from scan 2 to 15 is about 0.067. The phase transition from H1 to H2 for $LiNi_{0.8}Co_{0.2}O_2$ starts much earlier in the charging process than for $LiNiO_2$ in Fig. 2. All the Bragg peaks broadened and the peak separation becomes smaller compared to the spectra in Fig. 2. It is not very clear when the transition from H1 to H2 was completed. Ideally, we would like to identify another hexagonal phase H2a represented by the Bragg peaks in scan 9 as a transient phase between H1 and H2. However, we need to design more experiments and collect more *in situ* spectra to support this hypothesis. In Fig. 4, H2 single phase was marked on the curve for scan 12. It is based on the following reason: In Fig.5, before scan 11, the position of $(110)_{H2}$ peak continuously moves to higher angles after it had been formed in scan 5. However, after scan 11, the position of $(110)_{H2}$ peak turned around and moves to slightly lower angles until it reached its final position for H3 in scan 16. This interesting phenomenon is contributed by the Co atoms in the structure which will be discussed more in later publications. In this present paper, we use this turning point to identify the end of a phase transition. The lattice constants obtained from least square refinements are listed in Table I for H1 (using data from scan 1); in Table II for H2 (using data from scan 12); and in Table III for H3 (using data from scan 16). The most significant difference between the spectra in Fig. 4 and in Fig 2 is the phase transition from H2 to H3. In Fig. 2, the new $(003)_{H3}$ peak appears at about 15.2 ° which is far higher than $(003)_{H2}$ at 14.32 °. During the phase transition from H2 to H3 the position of $(003)_{H2}$ and $(003)_{H3}$ does not move much while the intensity of $(003)_{H3}$ grows in expense of $(003)_{H2}$. However, in Figure 4, the transition from H2 to H3 is progressed in a quasi-continuous manner. Therefore, although at the end of transition, the lattice constant "c" of H3 in Fig. 4 is smaller than that in fig. 2 (13.243 Å vs 13.354 Å), the "c" axis of H3 for $LiNi_{0.8}Co_{0.2}O_2$ in Fig. 4 is larger than that for $LiNiO_2$ in Fig. 2 at 4.5 V (about 13.5 Å vs 13.4 Å).

Figure 6 shows the first charging curve of the *in situ* cell using $LiNi_{0.75}Mg_{0.125}Ti_{0.125}O_2$ cathode (20.9 mg active material) when charged at a constant current (0.5 mA at C/12 rate) between 2.85 V to 5.2 V. The initial voltage jumped to 4.32 V and then relaxed to about 4.0 V, form one plateaus at 4.0 V and then rise continuously to 5.2 V. The *in situ* XRD spectra are plotted in Fig. 7 for (003) peak region and Fig. 8 for (101) to (113) region. The first scan was started before charge current applied to the cell with open circuit voltage of 2.85 V. The charging current was applied to the cell after the 2θ scan passed 16 degree. The last scan was taken during the last part of the charging towards 5.2 V. The numbers corresponding to XRD scans in Fig. 7 and 8 are marked on the charging curve in Fig. 6. Each scan took about 1.1 hour and the increment of x value in $Li_{1-x}Ni_{0.75}Mg_{0.125}Ti_{0.125}O_2$ in the consequent scans from scan 1 to 15 is about 0.091. It has been demonstrated by Gao[1] that the improvement in thermal stability for $LiNi_{0.8}Co_{0.2}O_2$ is not very impressive compared to the undoped $LiNiO_2$. The reduction in shrinkage of "c" axis at about 4.5 V for $LiNi_{0.8}Co_{0.2}O_2$ is also non-significant compared to $LiNiO_2$. This is in good agreement with the hypothesis by Ohzuku and us that the collapse of "c" axis is responsible for the poor thermal stability. In contrast with the result of $LiNi_{0.8}Co_{0.2}O_2$, the improvement in thermal stability is dramatic for $LiNi_{0.75}Mg_{0.125}Ti_{0.125}O_2$ compared to $LiNiO_2$. Quite interestingly, the formation of H3 phase is completely suppressed in Fig. 7 and 8 for $LiNi_{0.75}Mg_{0.125}Ti_{0.125}O_2$. Although

there might be a H2a transient phase formed from scan 3 to scan 8. There is no indication of H3 phase formation with lattice constant "c" smaller than 14.0 Å at all. Even when the voltage was charged to as high as 5.2 V, the lattice constant "c" of H2 phase retained at a value as large as 14.60 Å. After repeated charging with small current and holding the voltage at 5.2 V, no signs of H3 phase formation can be detected. This is a strong evidence to support the hypothesis about the relationship between the poor thermal stability and formation of H3 phase with small lattice constant "c". The lattice constants obtained from least square refinements are listed in Table IV for H1 (using data from scan 1) and in Table V for H2 (using data from scan 11)

CONCLUSION

Using synchrotron x-ray source for in situ XRD studies provides a new powerful tool for studying the structural changes during cycling. For the $LiNiO_2$ based cathode materials, suppressing formation of the hexagonal phase H3 with small lattice constant "c" (less than 14 Å) at a fully charged state could improve the thermal stability. The new material synthesized by FMC with superior thermal stability is a good example of successful suppression of the H3 phase by doping.

ACKNOWLEDGMENT

This work was supported by the U. S. Department of Energy Division of Materials Science of the Office of Basic Energy Sciences, and the Office of Energy Research, Laboratory Technology Research Program, Under Contract No. DE-AC02-98CH10886.

REFERENCES

1. Y. Gao, M. V. Yakovleva, and W. B. Ebner, *Electrochemical and Solid State Letters*, **1**, 117 (1998).
2. J. R. Dahn, E. W. Fuller, M. Obrovac, and U. von Sacken, *Solid State Ionics*, **69**, 265 (1994).
3. Z. Zhang, D. Fouchard, and J. R. Rea, *J. Power Sources*, **70**, 16(1998).
4. T. Ohzuku, A. Ueda, and M. Kouguchi, *J. of Electrochem. Society*, **142**, 4033 (1995).
5. T. Ohzuku, A. Ueda, M. Nagayama, Y. Iwakoshi, and H. Komori, *Electrochimica Acta*, **38**, 1159 (1993)
6. T. Ohzuku, A. Ueda, and M. Nagayama, *J. of Electrochem. Society*, **140**, 1862 (1993).
7. J. N. Reimers, and J. R. Dahn, *J. of Electrochem. Society*, **139**, 2091 (1992).
8. W. Li, J. N. Reimers, and J. R. Dahn, *Solid State Ionics*, **67**, 123 (1993).
9. G. G. Amatucci, J. M. Tarascon, and L. C. Klein, *J. of Electrochem. Society*, **143**, 1114 (1996).
10. X. Q. Yang, X. Sun, and J. McBreen, Electrochemistry Communications (accepted and will appear soon at http://www.chemweb.com/ecos/elcomm.)
11. S. Mukerjee, T. R. Thurston, N. M. Jisrawi, X. Q. Yang, J. McBreen, M. L. Daroux, and X. K. Xing, *J. of Electrochem. Society*, **145**, (1998), 466.

Table I. Observed and calculated d-spacing for H1 hexagonal unit cell of $LiNi_{0.8}Co_{0.2}O_2$

(hkl)	$2\theta_{obs}$	d_{obs} (Å)	d_{calc} (Å)	Delta d (Å)
(003)	14.51	4.731	4.730	0.0012
(101)	28.27	2.447	2.448	-0.0010
(006)	29.27	2.365	2.365	-0.0002
(102)	29.51	2.346	2.345	0.0008
(104)	34.15	2.035	2.035	-0.0004
(105)	37.29	1.869	1.870	-0.0006
(107)	44.70	1.571	1.571	0.0005
(108)	48.90	1.444	1.444	-0.0001
(110)	49.22	1.435	1.435	0.0001
(113)	51.60	1.373	1.373	-0.0001
$\lambda = 1.195$ Å		a = 2.869 Å	c = 14.190 Å	

Table II. Observed and calculated d-spacing for H2 hexagonal unit cell of $LiNi_{0.8}Co_{0.2}O_2$

(hkl)	$2\theta_{obs}$	d_{obs} (Å)	d_{calc} (Å)	Delta d (Å)
(003)	14.43	4.757	4.750	0.0079
(101)	28.82	2.401	2.400	0.0011
(006)				
(102)	30.10	2.301	2.304	-0.0028
(104)	34.52	2.014	2.010	0.0037
(105)	37.60	1.854	1.851	0.0030
(107)	44.95	1.563	1.562	0.0014
(108)	49.18	1.436	1.437	-0.0016
(110)	50.31	1.406	1.406	0.0000
(113)	52.65	1.347	1.348	-0.0005
$\lambda = 1.195$ Å	a = 2.811 Å	c = 14.249 Å		

Table III. Observed and calculated d-spacing for H3 hexagonal unit cell of $LiNi_{0.8}Co_{0.2}O_2$

(hkl)	$2\theta_{obs}$	d_{obs} (Å)	d_{calc} (Å)	Delta d (Å)
(003)	15.60	4.403	4.414	-0.0119
(101)	28.82	2.401	2.401	0.0004
(006)				
(102)	30.25	2.290	2.291	-0.0008
(104)	35.40	1.965	1.965	0.0003
(105)	38.90	1.794	1.795	-0.0008
(107)	47.10	1.495	1.495	0.0000
(108)	51.70	1.370	1.370	0.0002
(110)	50.15	1.410	1.410	0.0003
(113)	52.85	1.343	1.343	-0.0002
$\lambda = 1.195$ Å	a = 2.819 Å	c = 13.243 Å		

Table IV. Observed and calculated d-spacing for H1 hexagonal unit cell of $LiNi_{0.75}Mg_{0.125}Ti_{0.125}O_2$

(hkl)	$2\theta_{obs}$	d_{obs} (Å)	d_{calc} (Å)	Delta d (Å)
(003)	15.41	4.764	4.763	0.0012
(101)	28.02	2.468	2.467	0.0011
(006)	29.09	2.379	2.381	-0.0022
(102)	29.30	2.362	2.364	-0.0011
(104)	33.88	2.051	2.051	-0.0001
(105)	37.00	1.883	1.884	-0.0005
(107)	44.38	1.582	1.582	-0.0002
(108)	48.50	1.455	1.454	0.0006
(110)	48.80	1.446	1.446	0.0003
(113)	51.18	1.383	1.384	-0.0003
$\lambda = 1.195$ Å	$a = 2.892$ Å	$c = 14.288$ Å		

Table V. Observed and calculated d-spacing for H2 hexagonal unit cell of $LiNi_{0.75}Mg_{0.125}Ti_{0.125}O_2$

(hkl)	$2\theta_{obs}$	d_{obs} (Å)	d_{calc} (Å)	Delta d (Å)
(003)	14.68	4.677	4.680	-0.0035
(101)	28.60	2.419	2.417	0.0021
(006)				
(102)	29.90	2.316	2.316	-0.0001
(104)	34.58	2.010	2.011	-0.0007
(105)	37.70	1.849	1.848	0.0016
(107)	45.25	1.553	1.553	0.0002
(108)	49.50	1.427	1.428	-0.0003
(110)	49.90	1.416	1.417	-0.0001
(113)	52.30	1.356	1.356	-0.0001
$\lambda = 1.195$ Å	$a = 2.833$ Å	$c = 14.041$ Å		

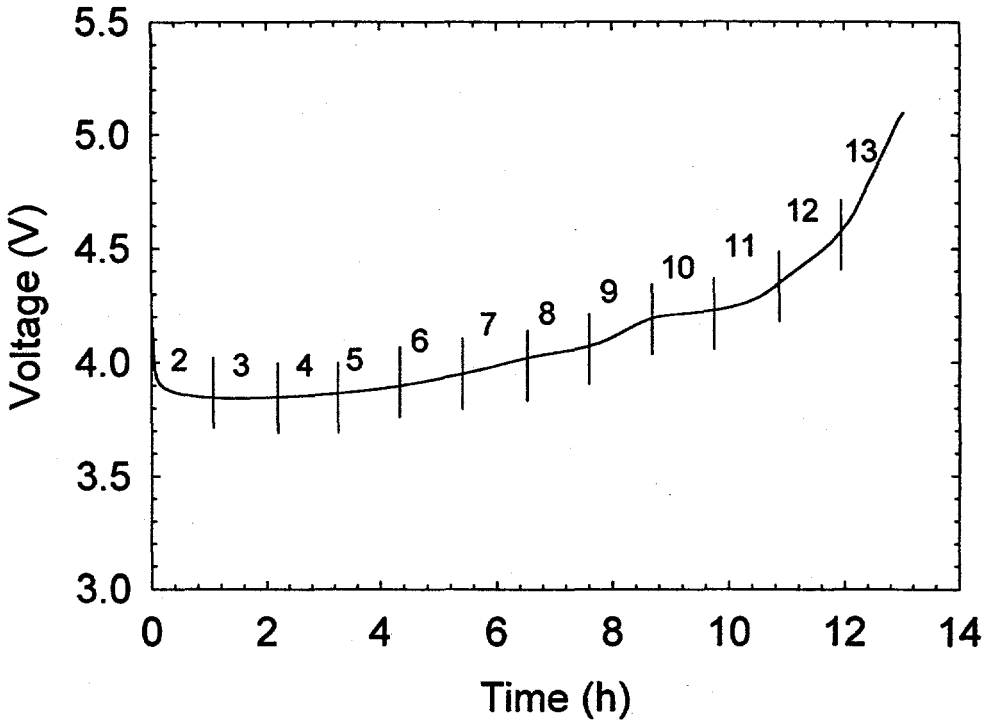

Figure 1 The first charging curve of a Li/$Li_{1-x}NiO_2$ cell at the C/13 rate from 3.5 to 5.1 V.

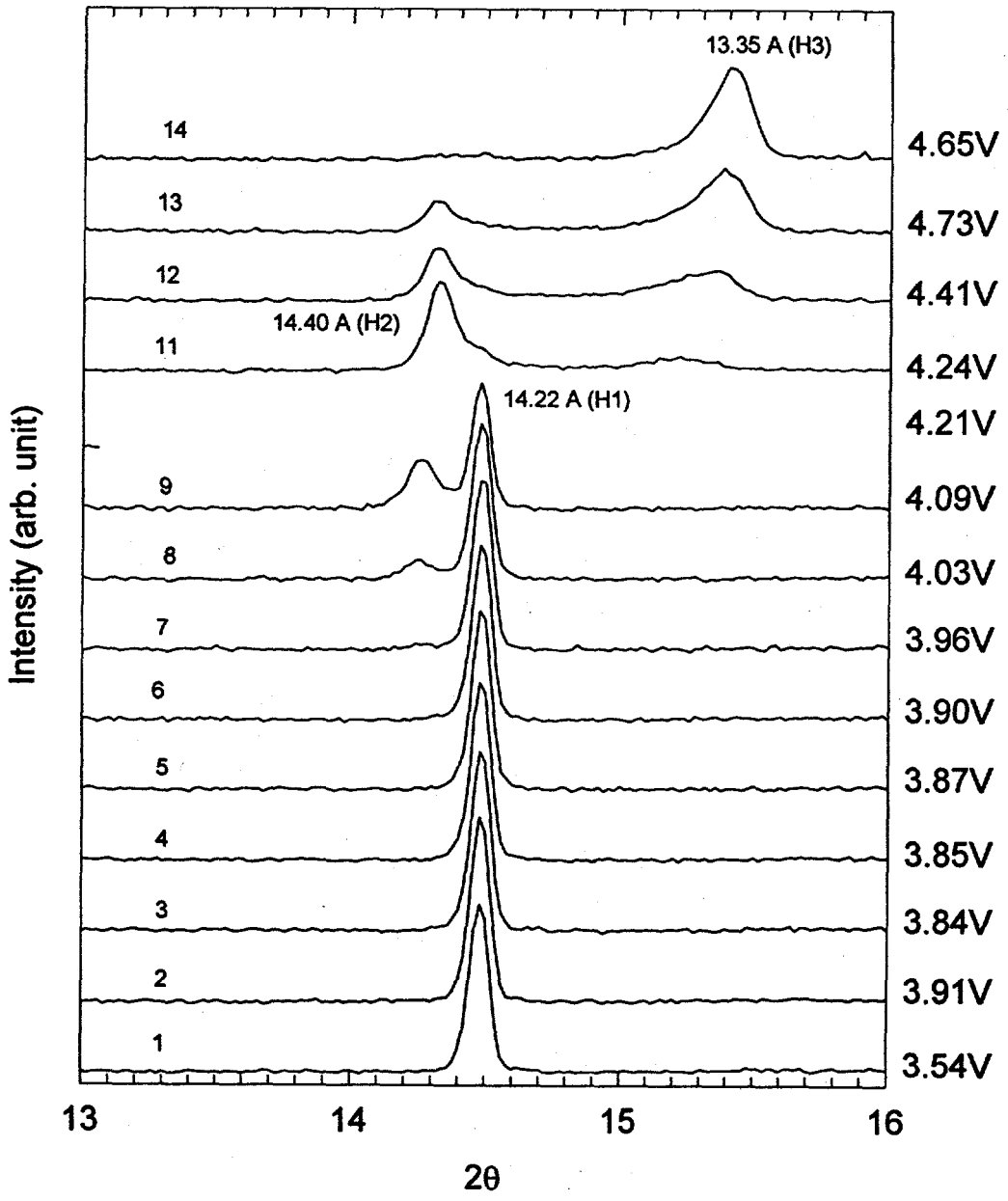

Figure 2 *In situ* XRD patterns of a $Li_{1-x}NiO_2$ cathode in the (003) region of the hexagonal structure during first charge at the C/13 rate from 3.5 to 5.1 V, 66 min for each 2θ scan from 13° to 54° (λ=1.195 Å).

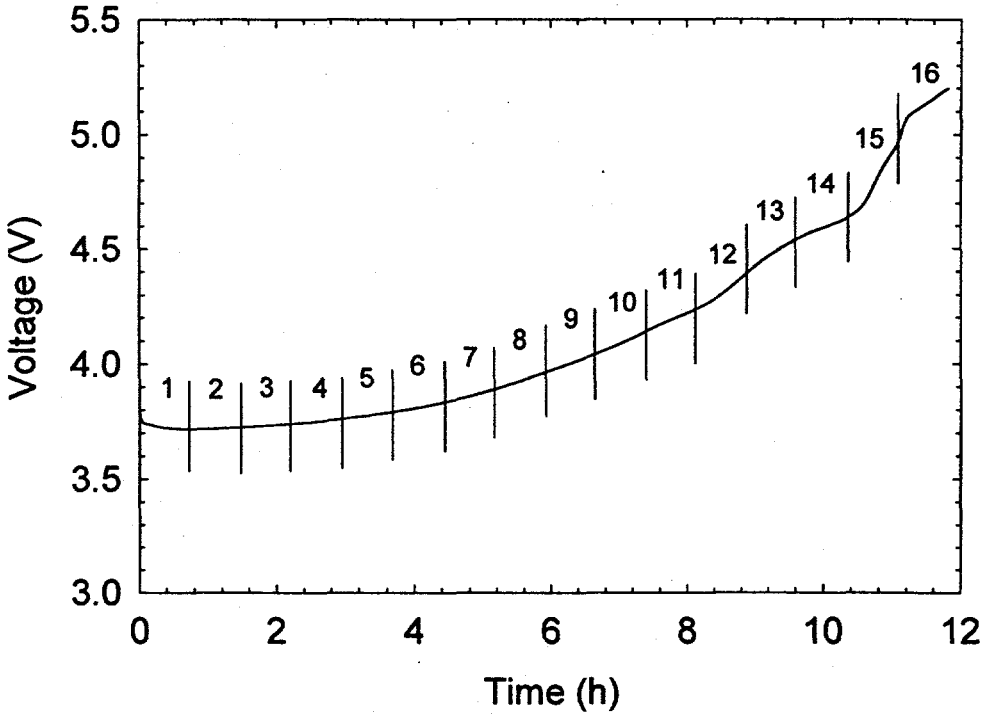

Figure 3 The first charging curve of a Li/ $LiNi_{0.8}Co_{0.2}O_2$ cell at the C/12 rate from 3.3 to 5.2 V

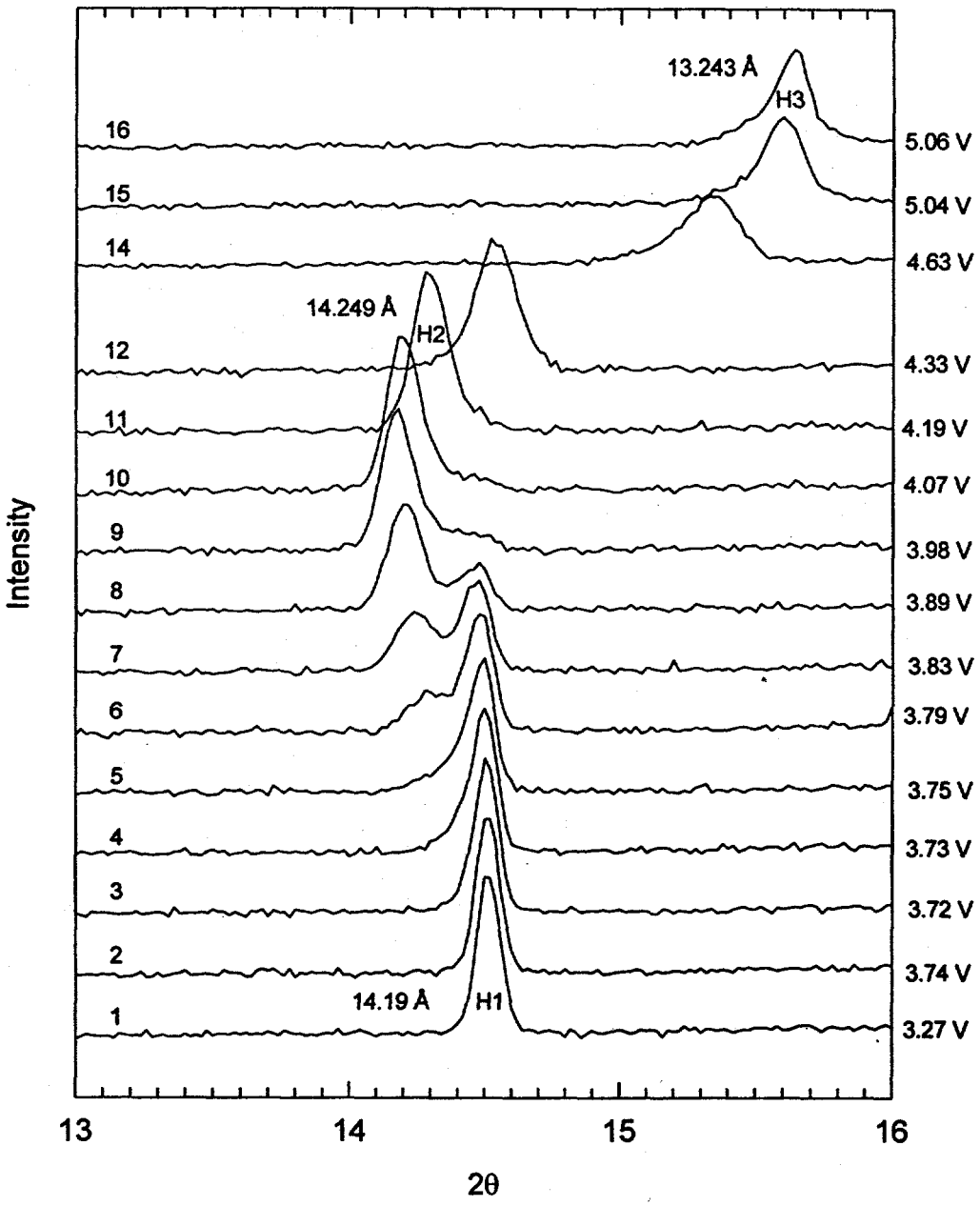

Figure 4 *In situ* XRD patterns of a $LiNi_{0.8}Co_{0.2}O_2$ cathode in the (003) region of the hexagonal structure during first charge at C/12 rate from 3.3 to 5.2 V. 0.8 hours for each 2θ scan from 13° to 54° (λ=1.195 Å).

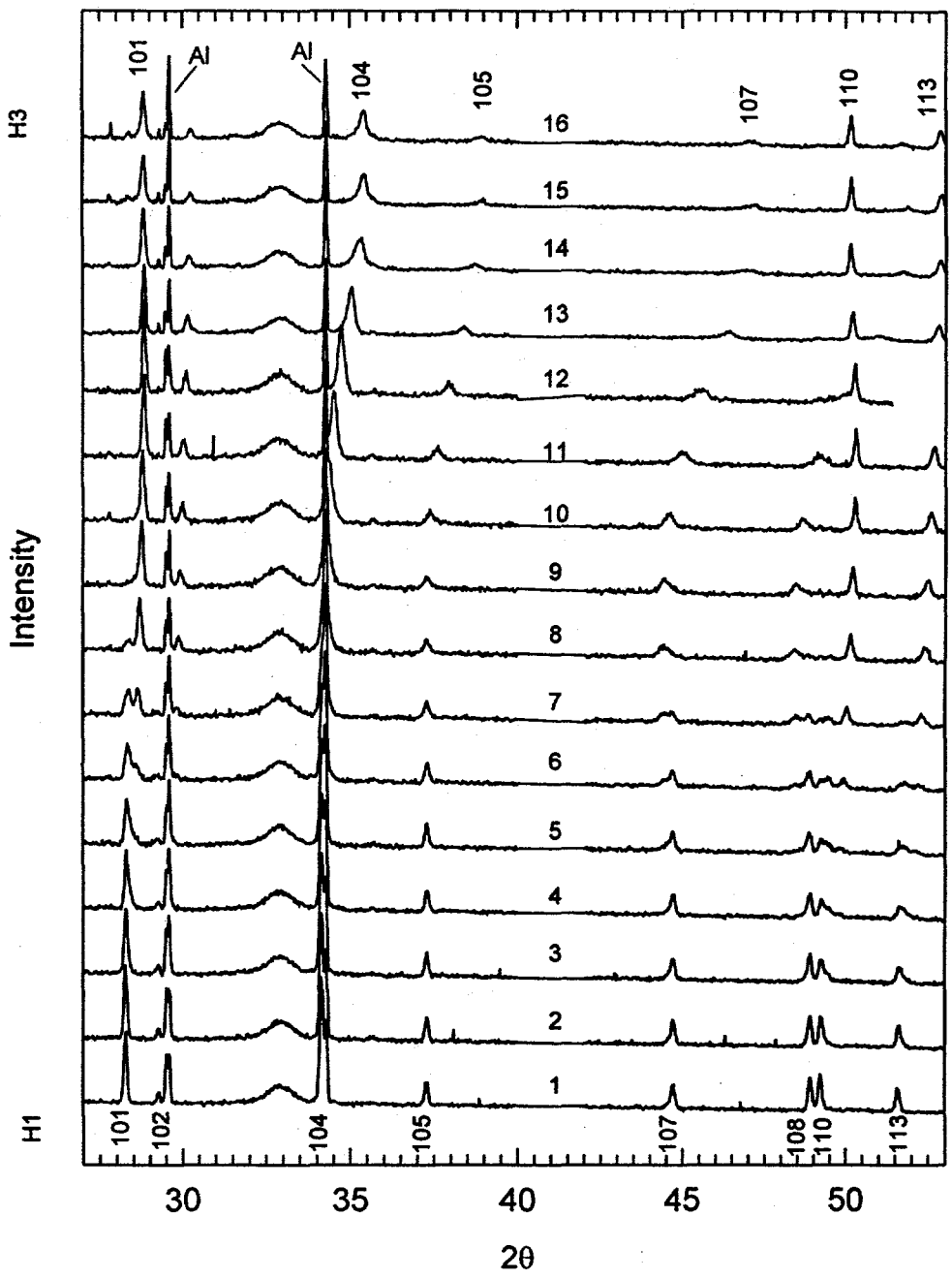

Figure 5 *In situ* XRD patterns of a $LiNi_{0.8}Co_{0.2}O_2$ cathode in the (101) to (113) region of the hexagonal structure during first charge at C/12 rate from 3.3 to 5.2 V. 0.8 hours for each 2θ scan from 13° to 54° (λ=1.195 Å).

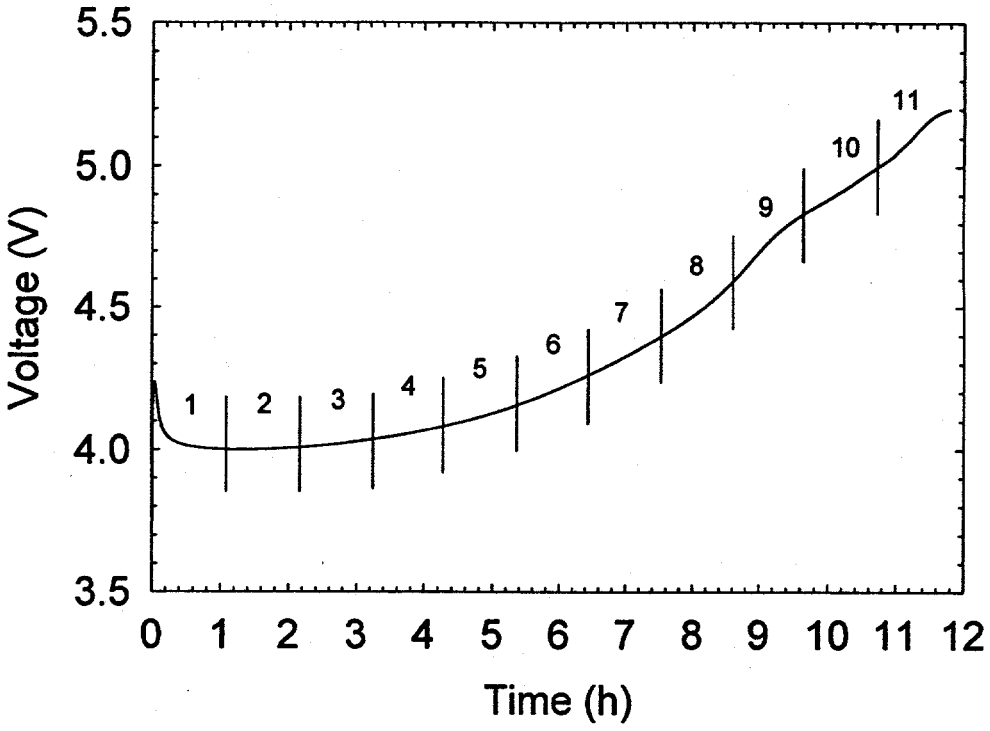

Figure 6 The first charging curve of a Li/ $LiNi_{0.75}Mg_{0.125}Ti_{0.125}O_2$ cell at the C/12 rate from 2.85 to 5.2 V.

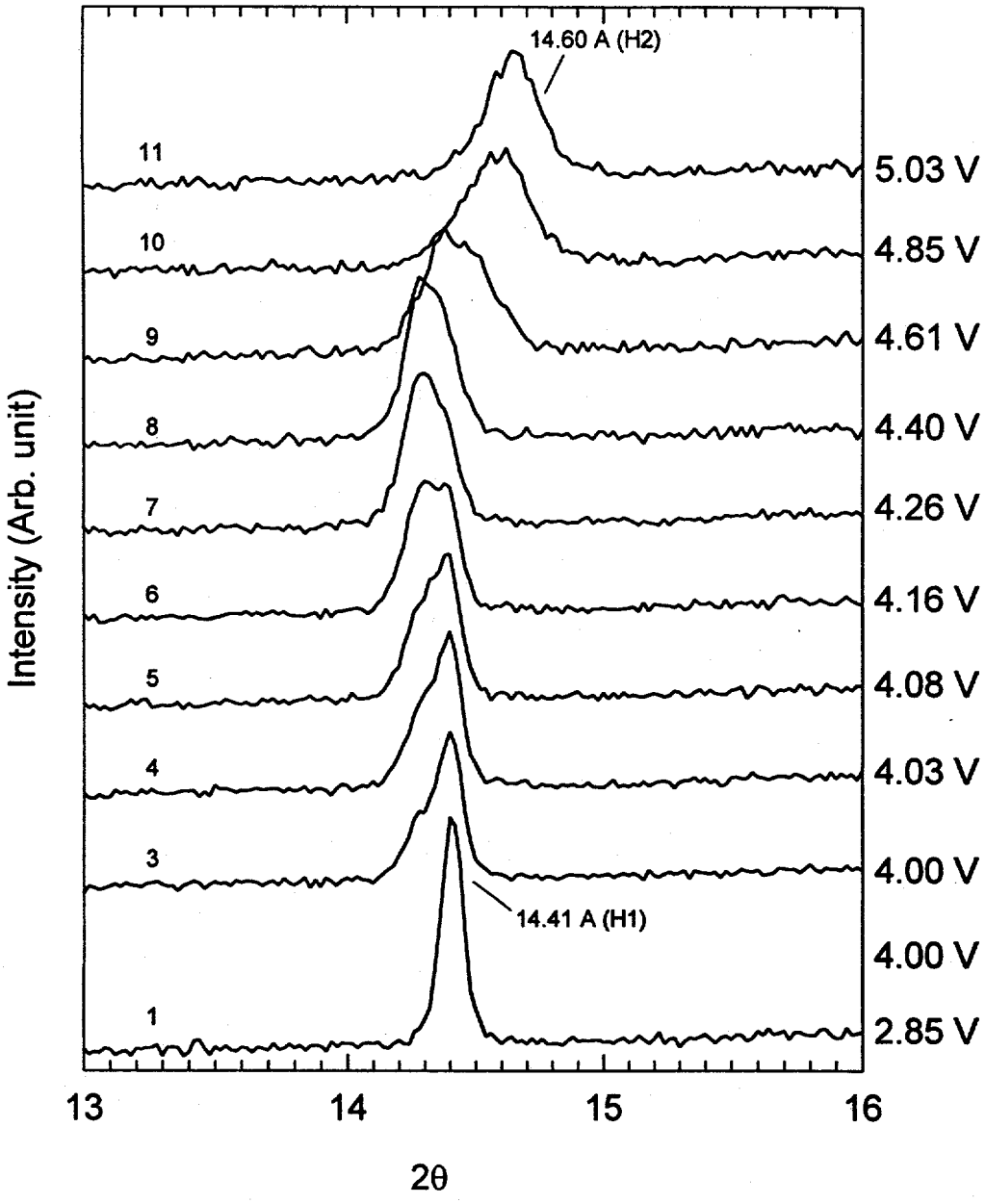

Figure 7 *In situ* XRD patterns of a $LiNi_{0.75}Mg_{0.125}Ti_{0.125}O_2$ cathode in the (003) region of the hexagonal structure during first charge at C/12 rate from 2.85 to 5.2 V. 1.1 hours for each 2θ scan from 13° to 54° (λ=1.195 Å).

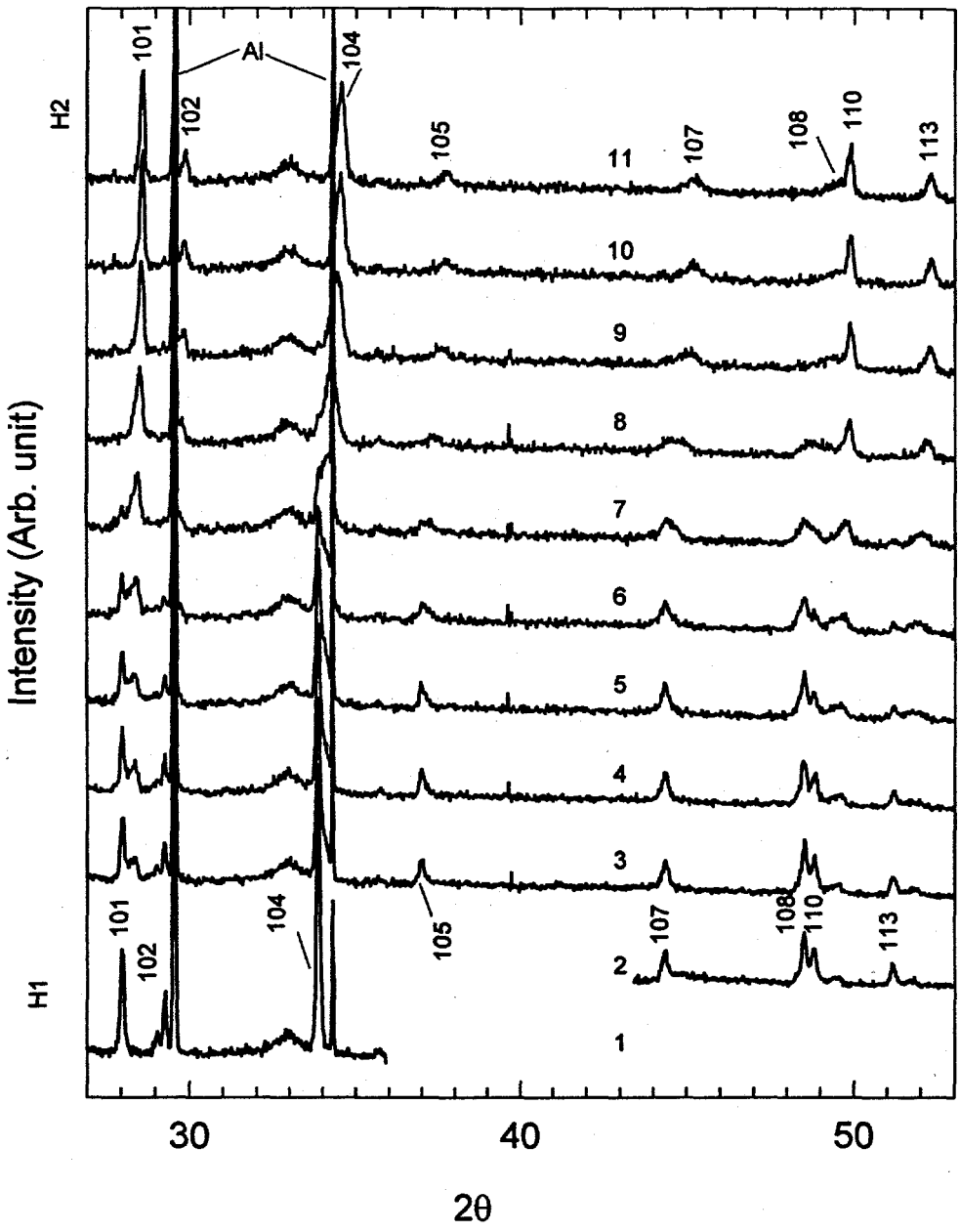

Figure 8 *In situ* XRD patterns of a $LiNi_{0.75}Mg_{0.125}Ti_{0.125}O_2$ cathode in the (101) to (113) region of the hexagonal structure during first charge at C/12 rate from 2.85 to 5.2 V. 1.1 hours for each 2θ scan from 13° to 54° (λ=1.195 Å).